Materials Research Society Symposium C
San Francisco, CA, Apr. 17-20, 1995

LUMINESCENCE IN Si/STRAINED $Si_{1-x}Ge_x$ HETEROSTRUCTURES

J.C. STURM, A. ST. AMOUR, Y. LACROIX*, AND M.L.W. THEWALT*
Department of Electrical Engineering, Princeton University
Princeton, NJ 08544 USA

*Department of Physics, Simon Fraser University
Burnaby, BC V5A1S6 Canada

ABSTRACT

This paper quickly reviews the structure of band-edge luminescence in Si/strained $Si_{1-x}Ge_x$ heterostructures, and then focusses on two recent developments -- the origin of "deep" sub-bandgap luminescence which is sometimes observed in structures grown by Molecular Beam Epitaxy (MBE) and the understanding of the temperature dependence of the band-edge luminescence (up to room temperature). Strong evidence will be presented that the origin of the deep luminescence is radiation damage, and that generated defects are segregated or trapped in the $Si_{1-x}Ge_x$ layers. The modelling of the temperature dependence by two-carrier numerical simulation is presented for the first time. The work and experimental data show convincingly that the strength of the luminescence at high temperature is controlled by recombination at the top silicon surface, which in turn can be controlled by surface passivation. At high pump powers and low temperatures, Auger recombination reduces the lifetime in the $Si_{1-x}Ge_x$ layers, and leads to a luminescence vs. temperature which is flat up to 250 K and which is reduced only by a factor of three at room temperature.

INTRODUCTION

Luminescence in Si/strained $Si_{1-x}Ge_x$ heterostructures is of interest for two reasons. First, photoluminescence is a valuable scientific probe into the band-edge structure of such $Si/Si_{1-x}Ge_x/Si$ quantum wells and their interfaces. Phenomena such as the bandgap, quantum confinement, and band offset type may all be probed through photoluminescence. Second, there is a great hope that the development of the Si/Ge material system will lead to an efficient silicon-based electrically-pumped light emitter. In this paper, band-edge luminescence in $Si_{1-x}Ge_x/Si$ structures on (100) Si substrates will be briefly reviewed, and then two recent research issues will be explored. We show strong evidence that the "deep" luminescence in such $Si_{1-x}Ge_x$ structures grown by solid-source MBE is the result of radiation damage occurring during the growth process. Second, the temperature dependence of the luminescence in $Si/Si_{1-x}Ge_x/Si$ quantum wells will be analyzed by two-carrier numerical simulation for the first time. It will be shown that passivation of the top silicon surface is vital for obtaining strong luminescence at high temperature, and that under conditions of high pump power, a luminescence which is constant up to 250 K can be observed.

Mat. Res. Soc. Symp. Proc. Vol. 379 © 1995 Materials Research Society

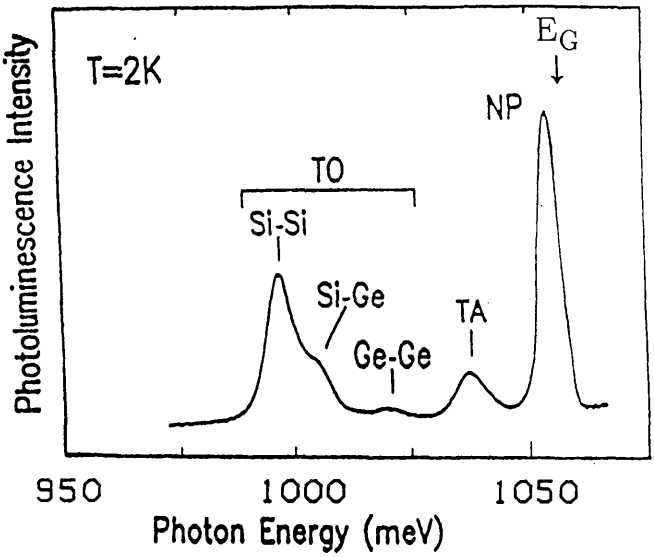

Fig. 1. 2 K photoluminescence of a sample with 10 strained $Si_{0.84}Ge_{0.16}$ 3-nm quantum wells separated by 6-nm Si barriers.

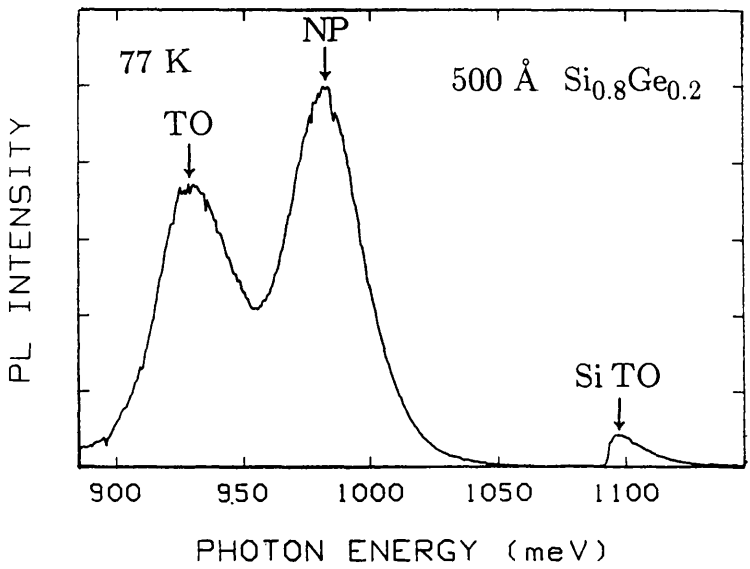

Fig. 2. 77 K photoluminescence of a single 50-nm strained $Si_{0.8}Ge_{0.2}$ layer (with a silicon cap). Note the clear evidence of no-phonon (NP) and transverse optical phonon replica (TO) peaks.

BAND-EDGE LUMINESCENCE SPECTRA

Strained $Si_{1-x}Ge_x$ alloys on Si (100) substrates with small x (e.g. < 0.5) have a band structure similar in many ways to that of silicon. Although the strain splits the band-edge degeneracies present in silicon, the band-edge structure of the alloys (strained and unstrained) is still indirect, with the conduction band minima lying at the Δ points and the valence band maximum at the zone center. At low temperatures, the photoluminescence (PL) is due to the radiative recombination of excitons, and to conserve the crystal momentum a phonon is commonly emitted. PL spectra of Si-rich alloys were first observed in unstrained material [1,2] and are similar to that of silicon, but with three major exceptions. First, the spectral features are shifted to lower energy because of the lower bandgap of the alloys. Second, although the PL associated with the emission of a transverse acoustic (TA) phonon is similar to that in silicon, the component associated with the emission of a transverse optical phonon (TO) is split into three components because of the three possible nearest neighbor interactions (Si-Si, Si-Ge, and Ge-Ge). Finally, a relatively strong no-phonon (NP) PL line is observed in the neighborhood of the bandgap (decreased by an exciton energy). The strong NP line results not just from the weak effect of the localization of excitons on shallow impurities at low temperatures as in silicon (bound excitons), but results predominately from the alloy randomness. This randomness breaks the translational symmetry of the crystal, so that the crystal momentum no longer must be strictly conserved. Hence transitions directly from the conduction band minima to the valence band maximum are now allowed, even though the material still has an indirect bandgap.

The first report of band-edge luminescence in a strained $Si_{1-x}Ge_x$ alloy on Si was by Terashima et al in 1990 [3]. The $Si_{1-x}Ge_x$ layer contained only 4% Ge, was relatively thick (0.5 μm), and was without a Si capping layer. In 1991, the first band-edge PL in samples with a higher Ge concentration ($x = 0.16$) and in quantum wells was reported [4]. A typical spectrum similar to that reported in Ref. 4 ($x = 0.16$ and 10 quantum wells of width 3 nm, with 6 nm Si layers between the QW's) is shown in Fig. 1. The three-fold splitting of the TO phonon line is clearly evident, as well as the weaker TA phonon replica. Also note the NP line in the region of the bandgap as described above. Except for a different bandgap, to first order the band-edge PL in unstrained alloys and strained alloys (and quantum wells) is similar.

Fig. 2 shows the PL spectrum of a single $Si_{0.8}Ge_{0.2}$ layer of thickness 50 nm, capped with a Si layer, measured at 77 K. At 77 K, excitons are no longer bound to impurities, and with a single 50 nm layer, there can clearly be no quantum confinement effects. Although the higher temperature broadens the lines present in the low temperature spectrum of Fig. 1, the TO and NP contributions are still clearly present. This unambiguously shows that the origin of the NP PL line is not related to low temperature localization or any quantum confinement or superlattice effects, and that it is due to a bulk phenomenon, such as the alloy randomness discussed above.

Although this band-edge PL in quantum wells was first observed in layers grown by Rapid Thermal Chemical Vapor Deposition (RTCVD) [4,5], it has also now been observed in layers grown by solid-source and gas-source MBE under proper conditions [6,7]. The band-edge luminescence has been used to probe such effects as the bandgap of strained layers vs. Ge content and quantum confinement effects [8,9].

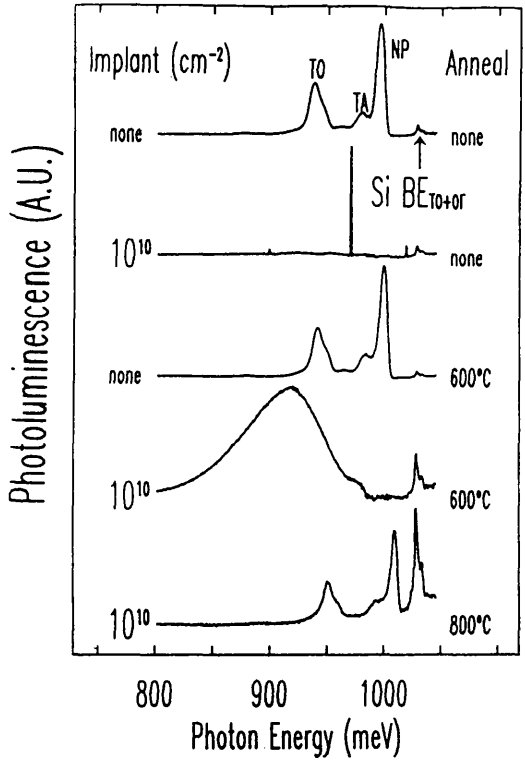

Fig. 3. 2 K photoluminescence of a single strained $Si_{0.8}Ge_{0.2}$ 6-nm quantum well with a 15-nm Si cap for various implantation doses of 50 keV Si^{29+} and annealing conditions (10 min in N_2).

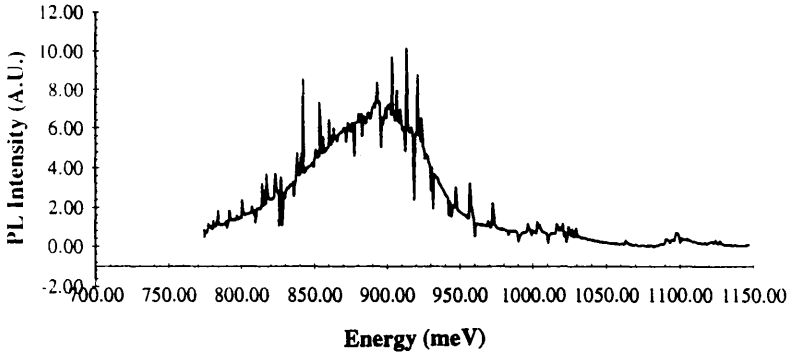

Fig. 4. 77K photoluminescence of a sample similar to that of Fig. 3, except for a 100-keV H^+ implant with a dose of 10^{15} cm^{-2} and a 10 min 600 ° C anneal.

"DEEP" LUMINESCENCE

Before band-edge luminescence in strained layers had been reported, a deep luminescence of unknown origin had been reported in layers grown by solid-source MBE [10]. The characteristic features of this luminescence are a peak energy about 80 - 120 meV below the bandedge and a peak width on the order of 100 meV. The luminescence is sometimes seen as grown, but sometimes first requires an annealing step at roughly 600 °C. In some samples, annealing at 700 °C or higher destroys this deep luminescence, and band-edge luminescence can actually appear after this high temperature annealing [11]. This deep luminescence is observed without any extended defects, such as dislocations. Possible theories for the origin of this deep luminescence have included donor-acceptor pairs [12], optically active defects [11], and Ge-rich interstitial platelets [13]. To the best knowledge of the authors, however, this deep luminescence has not been observed in as-grown CVD layers without defects (ie. dislocations). In any case this center has aroused extreme interest because of the very high reported initial quantum efficiencies (up to 30% [10]), although it appears these efficiencies decrease over time.

To probe the physical origin of this center, we attempted to introduce such luminescence into single quantum well samples with x = 0.10 to 0.25 grown by RTCVD, which as-grown all exhibited band-edge luminescence as in Fig. 1. The well thicknesses were 90 nm for x = 0.1 and under 10 nm for larger x, and all wells were capped with a 15 nm Si layer. The samples were subjected to a 50 keV ion implant of Si^{29+} ions at low doses to create radiation damage. After annealing at 600 °C for 10 min in nitrogen, the samples indeed exhibited a deep luminescence similar to that reported in samples grown by MBE [14] (Fig. 3). Unimplanted control samples which were annealed simultaneously still exhibited band-edge luminescence, so that furnace contamination can be ruled out as the sole cause of the deep luminescence. Besides the peak position and the peak width, the dependence of the peak intensity on the PL measurement temperature and excitation pump power were also similar to that of the deep PL seen in MBE-grown samples. Furthermore, annealing at 800 °C destroyed the deep luminescence, and the original band-edge luminescence was recovered, similar to the behavior of the deep luminescence in the MBE samples. Therefore, we conclude that the center responsible for the deep PL is the same in the MBE-grown samples, and that this center is created through radiation damage.

The experiments were repeated with hydrogen implantation (100 keV, H^+) for x = 0.2. No deep luminescence was observed for a dose of 3 x 10^{12} cm^{-2}, but a similar deep luminescence was observed at 77 K after a 10 min 600 °C anneal for a dose of 10^{15} cm^{-2} (Fig. 4). That a larger dose is required for a hydrogen implant (with a mass much lighter than that of silicon) is consistent with the concept that radiation damage is responsible for the deep luminescence. Because of the very low dose of silicon implanted, implying an even lower potential dose of stray dopant ions in the ion implanter, and because of the ability to anneal out the deep PL at a relatively low temperature (800 °C), the donor-acceptor hypothesis as the origin of the deep luminescence is inconsistent with our results.

Fig. 5 shows a profile calculated using the TRIM program [15] of the implanted Si ions themselves as well as the resulting damage (vacancies and interstitials) for a 50 keV Si^{29+} implant. Note that while damage is directly created in $Si_{1-x}Ge_x$, damage is also created in the silicon layers. However, both in our experiments and those with MBE-grown samples, deep luminescence is only observed associated with strained $Si_{1-x}Ge_x$ layers, not with Si layers

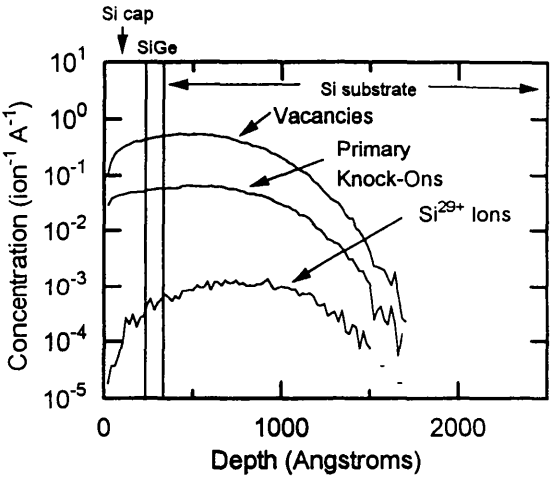

Fig. 5. TRIM calculation of implant distribution, vacancies, and knock-ons per implanted 50 keV Si^{29+} ion.

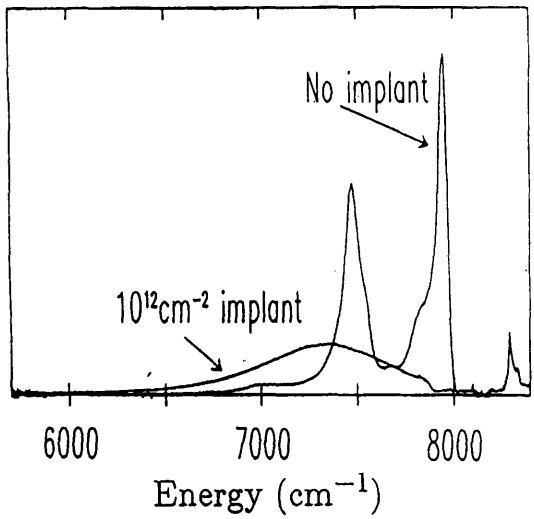

Fig. 6. 2 K photoluminescence of a sample similar to that of Fig. 3, except for a Si cap thickness of 300 nm. The implant and anneal were 50 keV Si^{29+} at 10^{12} cm^{-2} and 600 °C for 10 min in N_2.

grown under similar conditions. We then repeated our experiments for an x = 0.2 sample using a silicon cap with an approximate thickness of 300 nm. In this case, all direct implantation effects (implanted ions and damage) are confined well within the cap (as can be inferred from Fig. 5). In this case, however, deep luminescence could also be observed from the $Si_{1-x}Ge_x$, and no deep luminescence from silicon was observed (Fig. 6). Thus it appears that the damage from the ion implant can migrate, and is then segregated or captured in the $Si_{1-x}Ge_x$ wells. That the damage segregates to the $Si_{1-x}Ge_x$ layers explains why no deep PL from Si is seen in samples with $Si_{1-x}Ge_x$ layers. Why no deep PL is seen in all-Si samples (without $Si_{1-x}Ge_x$ layers), either in our experiments or those of solid-source MBE, might be explained by migration of the defects to the surface, where they would be annihilated, or deep into the substrate. The exact nature and structure of the defect responsible for the deep luminescence is not known at present, however.

If radiation damage is indeed the source of the deep luminescence, then a source of such radiation damage must be present in MBE machines. Ideally the source would not be a fundamental effect, as the results vary widely from machine to machine. Electron beam evaporators are commonly used for the Si and Ge sources in solid-source MBE machines. However, the energy of the electron beams (~ 5 keV) is too small to directly cause radiation damage in the semiconductor because of the small mass of electrons. None the less, stray electron beams can charge the substrate to a negative potential if it is not well grounded (which would vary from machine to machine). Furthermore, the evaporated Si and Ge atoms must pass through this electron beam, which could easily ionize some of the atoms, and the positive ions would then be accelerated towards the substrate, leading to the radiation damage. Note that only an extremely small fraction of the atoms in the growth beam would need to undergo such a process. We observed deep PL with a dose of only 10^{10} cm^{-2} at an energy of 50 keV, implying a dose of 10^{11} cm^{-2} would be sufficient for a substrate charged to 5 kV. By comparison, one monolayer alone requires a flux of 10^{15} cm^{-2} atoms. In support of this hypothesis, at this conference I.A. Buyanova et al [16] reported the effect of controlling the substrate bias in a solid-source MBE machine (with an e-beam evaporator) with a good substrate electrical contact and an external power supply. For negative substrate biases, which would attract positive ions, deep luminescence was indeed observed for biases on the order of 1kV. For positive biases, which would repel positive ions and hence avoid damage, band-edge luminescence and no deep luminescence was observed.

TEMPERATURE DEPENDENCE OF BAND-EDGE LUMINESCENCE

As the temperature increases, the integrated PL from $Si_{1-x}Ge_x$ quantum wells remains constant until a "knee" temperature, above which it decreases exponentially with an activation energy similar to the valence band offset [17] (Fig. 7). For example, for x = 0.2 and x = 0.3 knee temperatures between 100 K and 200 K have been observed in high quality samples grown by RTCVD. Previous phenomenological modelling [17] has explained the drop as occurring while most carriers were still in the $Si_{1-x}Ge_x$, and caused by a substantially lower lifetime in the Si layers than in the $Si_{1-x}Ge_x$. The analytical model, however, made the gross assumptions of constant lifetimes (independent of carrier densities) and no band-bending, and did not address p-n junctions within the structures. In reality all of the above assumptions are suspect, especially because of the expected collection of holes in the quantum well due to the large valence band offset.

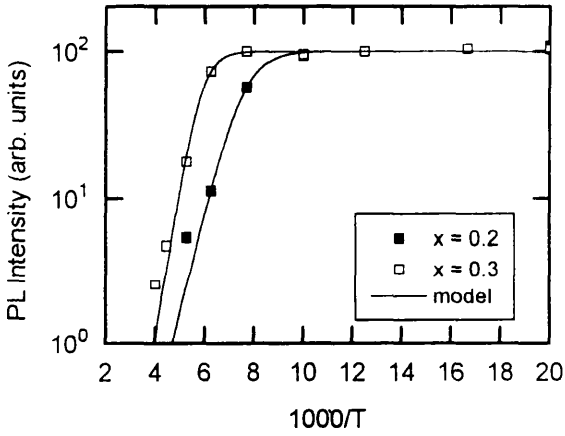

Fig. 7. Integrated luminescence vs. temperature for single $Si_{1-x}Ge_x$ quantum wells with x = 0.2 (15 nm thick) and 0.3 (5 nm thick) capped with 20 nm of Si (no passivation). The luminescence strength at low temperature is arbitrarily set to be the same in the two samples. The analytical model is described in Ref. 17.

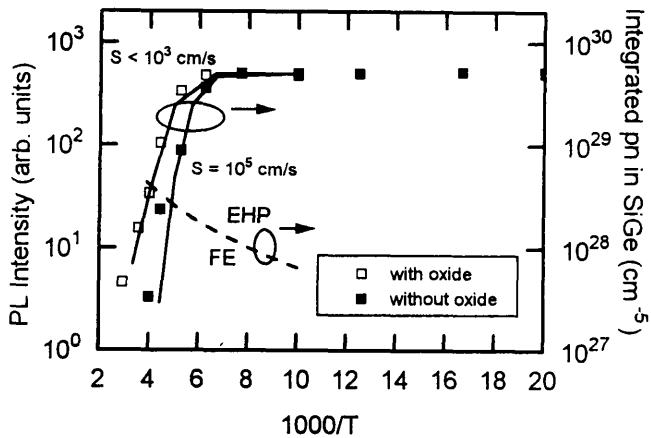

Fig. 8. Integrated photoluminescence data (points, left axis) and numerical model (lines, right axis) vs. temperature for the x = 0.3 quantum well of Fig. 7, both with and without passivating SiO_2 grown at 800 °C. The pump power density was 0.28 W/cm^2. The dashed line represents the expected transition between discrete excitons and an electron-hole plasma [20, 21].

To better understand the temperature dependence of luminescence, we have for the first time used a two-carrier device simulator (MEDICI [18]) to numerically solve for the carrier distribution profiles in the heterostructure during steady state carrier generation by a pump laser, and then related the carrier distribution to the photoluminescence. The program allows one to vary lifetimes, Auger recombination coefficients, temperature, pump power, absorption depth, etc. to find exact carrier distributions without making the simplifying assumptions required of an analytical model. In general, the relationship between the carrier densities and luminescence is not straightforward because of the complex relationship between exciton density, temperature, and carrier concentration [19]. However, for most of the conditions simulated, the carrier concentrations in the $Si_{1-x}Ge_x$ were high enough (above the Mott criteria), so that the exciton model is no longer valid and the luminescence can be thought of as originating from an electron-hole plasma [20, 21]. In this limit, regardless of temperature, the luminescence should be proportional to the p-n product. Therefore, the integrated p-n product across the quantum well was compared to the measured luminescence intensity vs. temperature.

The results are shown in Fig. 8 for a single quantum well with x = 0.3 (5 nm width) capped with 20 nm of Si. Because it seemed unreasonable that the lifetime in Si should be lower than that in the $Si_{1-x}Ge_x$, a low level injection lifetime of 1 μs was used in both materials. It was still possible to model the observed spectra, however, but only if a recombination velocity at the top silicon surface (unpassivated in this case) of 10^5 cm/s was assumed. This implies that the dominant non-radiative recombination (which controls the carrier density in the entire structure and the PL strength) was occurring at the top Si surface, not in the $Si_{1-x}Ge_x$. To passivate the surface, we oxidized the sample for 10 min in O_2 at 800 °C. This improved the SiGe PL at high temperature, and pushed the knee temperature from ~170 K to ~200 K. The PL could then be modelled with a surface recombination velocity below 10^3 cm/s, consistent with the passivation reducing the surface recombination. Actually, the unpassivated samples were obtained by removing the oxide with dilute HF from oxidized samples. This was done to ensure that all samples received the sample thermal treatment and to show unambiguously that the effect was due to surface passivation, and not thermal annealling.

The calculated band diagram and carrier concentrations vs. depth for the conditions of Fig. 8 (with oxide) at 200 K are shown in Fig. 9. Note that the quasi- fermi levels are flat throughout the region of the quantum well and deep into the substrate (which was doped p-type in this experiment). The flat quasi-fermi levels between the Si and the SiGe indicated a quasi-equilibrium between the carrier densities across the heterointerfaces. Note that the photogenerated carriers, which are generated within a few microns of the surface, are able to travel over 100 μm into the substrate (assuming a lifetime of 1 μs). Because the minority carriers can travel so far, the top surface's effect on the SiGe PL does not require a very thin Si cap (~25 nm in the above experiments). Increasing the cap thickness to 300 nm had no observable effect on either experiments or simulations.

We have also previously observed that at very high pump densities (28 W/cm^2), x = 0.3 samples with oxide had a knee temperature as high as 250 K and an integrated luminescence intensity which decreased by only a factor of 3 at room temperature [17]. This result could be phenomologically explained by either an increase of the effective lifetime in Si (reduced surface recombination velocity) or a decreased SiGe lifetime at high pump powers, but it was not possible to determine which was more likely with an analytical model. This problem was then examined with the numerical model (Fig. 10). Because of the high carrier densities in

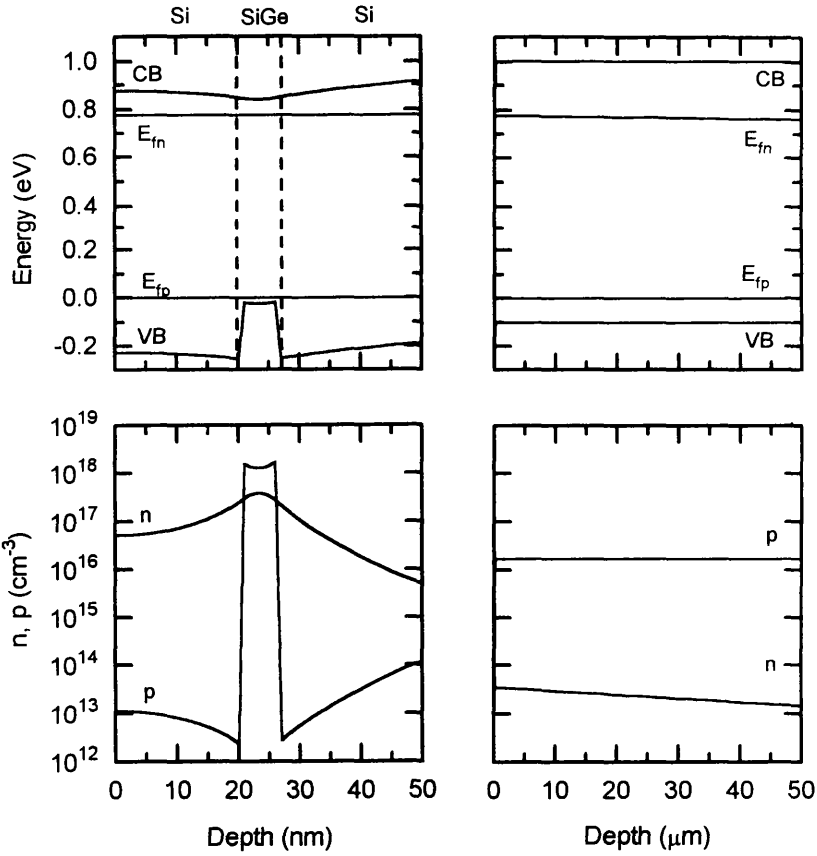

Fig. 9. Calculated band diagram and carrier concentration vs. depth for the x = 0.3 sample of Fig. 7 (passivated surface) at 200 K at a pump power density of 0.28 W/cm^2. On the 50 μm depth scale, the quantum well structure is not visible (all in top 0.1 μm).

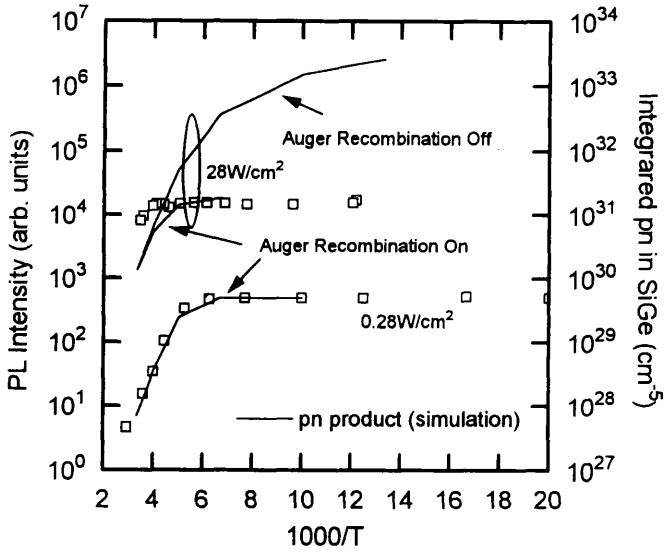

Fig. 10. Data and numerical modelling (with and without Auger recombination) for x = 0.3 (passivated surface) at high and low pump powers (0.28 vs 28 W/cm^2).

the SiGe (>> 10^{18} cm^{-3}) at high pump power and low temperature, Auger recombination was very important. This had the effect of reducing the lifetime in the SiGe by nearly one order of magnitude at low temperature, although it had no effect at high temperature when the carrier density in the SiGe well was much lower. Such modelling qualitatively showed the increase in the knee temperature as experimentally observed (Fig. 10) when going from a low to a high pump power. While we are convinced that this is the correct physical explanation for the observed phenomenon, no attempt was made to adjust the many variables in the MEDICI program to obtain better quantitative agreement between the experiment and the simulation.

SUMMARY

It has been shown that band-edge photoluminescence is a valuable probe for investigating $Si/Si_{1-x}Ge_x$ heterostructures. We have presented evidence which strongly shows that the deep luminescence sometimes observed in solid-source MBE samples is caused by radiation damage which segregates to the SiGe layers. The most likely cause of the radiation damage is acceleration of ionized Si or Ge atoms, which are accelerated towards a substrate charged by stray electron beams. The structure of the optically active defect is not known at present, however. Integrated luminescence which is constant from low temperatures up to 200 K (250 K at high pump powers) can be obtained in high quality samples. Achieving optimum

SiGe PL results at high temperature requires the top Si surface be well passivated to avoid excessive surface recombination, however. The application of two-carrier numerical device modelling was introduced for the first time, and shown to be a very valuable tool for understanding the temperature behavior of luminescence in complex structures.

This work was supported by ONR, NSF, and USAF Rome Lab. We also thank TMA for loaning us the MEDICI simulation program.

REFERENCES

1. G.S. Mitchard and T.C. McGill, Phys. Rev. B **25**, 5351 (1982).

2. J. Weber and M.I. Alonso, Phys. Rev. B **40**, 5683 (1989).

3. K. Terashima, M. Tajima, and T. Tatsumi, App. Phys. Lett. **57**, 1925 (1990).

4. J.C. Sturm, H. Manoharan, L.C. Lenchyshyn, M.L.W. Thewalt, N.L. Rowell, J.P. Noel, and D.C. Houghton, Phys. Rev. Lett. **66**, 1361 (1991).

5. J.C. Sturm, P.V. Schwartz, E.J. Prinz, and H. Manoharan, J. Vac. Sci. Tech. B **9**, 2011 (1991).

6. J. Spitzer, K. Thonke, and R. Sauer, H. Kibbel, H.-J. Herzog, and E. Kasper, App. Phys. Lett. **60**, 1729 (1992).

7. S. Fukatsu, H. Yoshida, A. Fujiwara, Y. Takahashi, and Y. Shiraki, Appl. Phys. Lett. **61**, 804 (1992).

8. D.J. Robbins, L.T. Canham, S.J. Barnett, A.D. Pitt, and P. Calcott, J. Appl. Phys. **71**, 1407 (1992).

9. X. Xiao, C.W. Liu, J.C. Sturm, L.C. Lenchyshyn, M.L.W. Thewalt, R.B. Gregory, and P. Fejes, Appl. Phys. Lett. **60**, 2135 (1992).

10. J.P. Noel, N.L. Rowell, D.C. Houghton, and D.D. Perovic, Appl. Phys. Lett. **57**, 1037 (1990).

11. K. Terashima, M. Tajima, N. Ikarashi, T. Niino, and T. Tatsumi, Jap. J. Appl. Phys. **30**, 3601 (1991).

12. E.R. Glaser, T.A. Kennedy, D.J. Godbey, P.E. Thompson, K.L. Wang, and C.H. Chern, Phys. Rev. B **47**, 1305 (1993).

13. J.P. Noel, N.L. Rowell, D.C. Houghton, A. Wang, and D.D. Perovic, Appl. Phys. Lett. **61**, 690 (1992).

14. J.C. Sturm, A. St. Amour, Y. Lacroix, and M.L.W. Thewalt, App. Phys. Lett. **64**, 2291 (1994).

15. TRIM provided by J. Ziegler, IBM Yorktown Research Center.

16. I.A. Buyanova, A. Henry, W.M. Chen, W.X. Ni, G.V. Hansson, and B. Monemar, Proc. Mat. Res. Soc. **379**, to be published (1995).

17. A. St. Amour, J.C. Sturm, Y. Lacroix, and J.C. Sturm, Appl. Phys. Lett. **65**, 3344 (1994).

18. MEDICI is a product of Technology Modelling Associates (TMA), Palo Alto, CA.

19. H. Schlangenotto, H. Maeder, and W. Gerlach, Phys. Stat. Sol. (a) **21**, 357 (1974).

20. N.F. Mott, *Metal Insulator Transitions*, (Taylor & Francis, New York, 1990).

21. X. Xiao, C.W. Liu, J.C. Sturm, L.C. Lenchyshyn, and M.L.W. Thewalt, Appl. Phys. Lett. **60**, 1720 (1992).